# 1C.4 THE IMPORTANCE OF LOW-DEFORMATION VORTICITY IN TROPICAL CYCLONE FORMATION

K. J. Tory*, R. A. Dare, S. S. Chand, N. E. Davidson, and J. L. McBride
Centre for Australian Weather and Climate Research, Melbourne, Australia

## 1. INTRODUCTION

Studies of tropical cyclone (TC) formation from tropical waves have shown that formation requires a wave-relative closed circulation: the "marsupial pouch" concept (Dunkerton et al. 2009). This results in a non-ventilated region of atmosphere in which the modification of moisture, temperature and vorticity profiles by convective and boundary layer processes occurs undisturbed. TCs develop near the centre of the pouch where the flow is in near solid body rotation. In this paper a reference-frame independent parameter is introduced that effectively measures the level of solid-body rotation in the lower troposphere. The parameter is the product of a normalized Okubo-Weiss parameter and absolute vorticity (OWZ). It is a simple diagnostic that can be used to identify vorticity rich regions of closed circulations.

We calculated OWZ in 20 years of ERA-interim re-analysis data and found that 95% of TCs in the global IBTrACS TC database had elevated values of OWZ on both the 850 and 500 hPa pressure levels at the time of TC declaration. This result led us to hypothesize that *All TC precursors contain enhanced OWZ*, and thus OWZ could be a very useful TC formation diagnostic. The clear OWZ signal in the relatively coarse reanalysis data associated with observed TCs suggests it could also be used in a TC detector for climate model applications.

OWZ is introduced in Section 2, and an argument is presented for why enhanced values are important for TC formation. In Section 3 the OWZ based TC detector is introduced and its performance when applied to the same 20 year period of ERA-interim reanalyses is described. In Section 4 the TC detector performance applied to a selection of CMIP3 climate models is presented.

## 2. LOW DEFORMATION VORTICITY

To determine the TC formation "sweet-spot" of Dunkerton et al. (2009), knowledge of the tropical wave phase speed is required, which makes it impossible to determine from instantaneous data. However, the Galilean invariant Okubo-Weiss (OW) parameter is enhanced surrounding all sweet-spots identified by Dunkerton et al. and subsequent papers by these authors.

OW is a measure of the relative amount of vorticity to deformation flow,

$$OW = \zeta^2 - \left(E^2 + F^2\right). \qquad (1)$$

Here $\zeta$ is the vertical component of relative vorticity, $E$ is the stretching deformation and $F$ is the shearing deformation. These quantities in Cartesian and cylindrical coordinates (Wang 2008) are,

$$\zeta = \left[\frac{\partial v}{\partial x} - \frac{\partial u}{\partial y}\right] = \left[\underline{\frac{\partial V}{\partial r}}_{SV} + \underline{\frac{V}{r}}_{CV} - \frac{1}{r}\frac{\partial U}{\partial \lambda}\right] \qquad (2a)$$

$$E = \left[\frac{\partial u}{\partial x} - \frac{\partial v}{\partial y}\right] = \left[\frac{\partial U}{\partial r} - \frac{U}{r} - \frac{1}{r}\frac{\partial V}{\partial \lambda}\right] \qquad (2b)$$

$$F = \left[\frac{\partial v}{\partial x} + \frac{\partial u}{\partial y}\right] = \left[\frac{\partial V}{\partial r} - \frac{V}{r} + \frac{1}{r}\frac{\partial U}{\partial \lambda}\right] \qquad (2c)$$

$u$ and $v$ are the zonal and meridional wind components, $x$ and $y$ are the zonal and meridional coordinate directions, $U$ and $V$ are the radial and tangential wind components, and $r$ and $\lambda$ are the radial and azimuthal coordinates. The subscripts *SV* and *CV* in Eq. 2a are included to demonstrate the similarity to shear and curvature vorticity in the natural coordinate system (e.g., Holton, 2004).

From Eq. 1 it can be seen that for a given vorticity, OW is maximized for zero deformation flow ($E = F = 0$, i.e., solid body rotation). Normalizing OW by dividing by the vorticity squared,

$$OW_{norm} = \left[\zeta^2 - \left(E^2 + F^2\right)\right] \big/ \zeta^2 \qquad (3)$$

yields a parameter that has a maximum value of one for solid body rotation, which can be used to identify zero deformation flow.

### 2.1 LDV FAVOURS TC FORMATION

Here we provide a simple theoretical argument for why TC formation may be favoured in a low deformation environment. We consider an axisymmetric ($\partial/\partial\lambda = 0$) and non-divergent ($U = 0$) circulation. Because the developing TC system vorticity tendency is greater in an environment of enhanced absolute vorticity[1] ($\eta = \zeta + f$) and because the balanced vortex spin-up is proportional to the inertial stability[2] ($I$), the most favourable location for TC formation will

[1] The dominant $\eta$-tendency term is equal to the horizontal inward flux of $\eta$.

[2] Solutions to the Sawyer Eliassen equations demonstrate greater efficiency in converting potential energy to kinetic energy with increasing $I$ (e.g., Shapiro and Willoughby 1982).

* *Corresponding author address*: Kevin J. Tory, CAWCR, GPO Box1289, Melbourne, Australia, 3001; e-mail: k.tory@bom.gov.au

be a finite region within the pouch where both $\eta$ and $I$ are largest. The inertial stability squared is given by,

$$I^2 = (\zeta + f)(2V/r + f). \quad (4)$$

To identify the most favourable formation region in our simplified axisymmetric pouch, we consider the streamline that contains the highest average vorticity and inertial stability. The area integrated vorticity inside a circular streamline of radius *r* is given by

$$\int 2\pi r \frac{1}{r}\frac{\partial(rV)}{\partial r} dr = 2\pi r V. \quad (5)$$

Dividing by the area of the closed streamline gives the area averaged vorticity, or vorticity concentration, within that streamline. Thus,

$$\bar{\zeta}(r) = 2V/r, \quad (6)$$

where the overbar represents the area average. It follows that the streamline containing the highest concentration of vorticity is the streamline with maximum $V/r$. A similar argument can be used to show that the area averaged $V/r$ and thus $I^2$ (Eq. 4) is greatest inside the maximum $V/r$ streamline when the flow is in solid body rotation.

A plot of *V* as a function of *r* for an axisymmetric circulation is depicted in Fig. 1 (blue curve). It shows *V* increasing with *r* up until the radius of maximum wind (RMW) and decreasing beyond that. Any straight line of positive gradient passing through the origin and intersecting the curve has a gradient equal to $V/r$ at the point (or points) of intersection. The gradient of the constant $V/r$ line that touches but does not cut the *V*-curve is equal to the maximum $V/r$ (Fig. 1, straight sloping line). Because this line touches at a tangent to the *V*-curve, $\partial V/\partial r = V/r$ at the intersection, which represents solid body rotation. In Fig. 1 the flow is in solid body rotation at $r = a$, which coincides with the maximum $V/r$. Thus the streamline containing the maximum area averaged vorticity lies at $r = a$ (Fig.1). Additionally, the maximum area averaged inertial stability inside this streamline occurs for solid body rotation (e.g., if *V* in Fig. 1 was defined by the thick purple line inside $r = a$). It follows that the most-favourable region for TC formation resides inside $r = a$ (shaded green in Fig. 1), and the flow is most favourable inside this region if it is in solid body rotation.

In this simplified environment *OW* reduces to,

$$OW = 4\frac{V}{r}\frac{\partial V}{\partial r}, \quad (6)$$

which means $OW$ and by definition $OW_{norm}$ decrease to zero at the radius of maximum wind (i.e., where $\partial V/\partial r = 0$), outside which the deformation exceeds the vorticity. Such environments are hostile to TC formation as developing vorticity anomalies will be sheared apart (e.g., Rozoff et al. 2006).

The two extremes of $OW_{norm}$ = 1 and 0 describe a formation favourability range of most favourable to hostile (shaded red in Fig. 1) respectively. Assuming the above TC formation favourability arguments are approximately valid for the non-axisymmetric and divergent, but still highly curved flows of typical TC formation regions the Galilean invariant Cartesian coordinate form of $OW_{norm}$ makes an ideal TC formation favourability scale parameter.

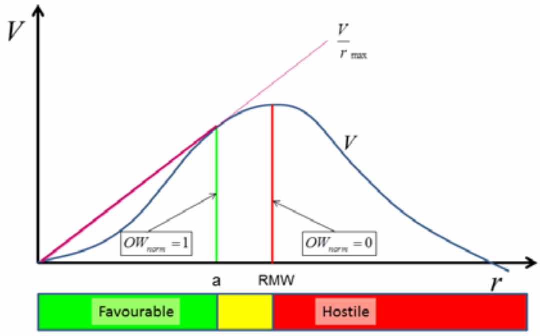


**Figure 1:** Schematic representation of a hypothetical tangential wind (*V*) profile (blue curve) with radius (*r*). The green and red lines depict the radius of maximum $V/r$ (*r*=a) and maximum wind (RMW).

### 2.2 LDV DIAGNOSTIC: OWZ

We choose to scale the absolute vorticity ($\eta$) with positive values of $OW_{norm}$ to get a quantity that reflects the solid body component of cyclonic absolute vorticity. We label the quantity OWZ, in recognition of the dominant contributions of the OW parameter and the vertical component of relative vorticity (with *Z* a Roman abbreviation of $\zeta$) thus,

$$OWZ = \max(OW_{norm}, 0) \times \eta \times sign(f). \quad (7)$$

Here the parameter is multiplied by the sign of *f* to ensure OWZ is positive and negative for cyclonic and anticyclonic flow curvature respectively in both hemispheres. It is clear from Eq. 7 that OWZ has the same magnitude as $\eta$ for solid body rotation, and is zero for flows in which $OW_{norm} = 0$ (e.g., zero curvature vorticity, or flows in which deformation exceeds vorticity).

## 3 OWZ TC FORMATION PREDICTOR

Experimentation with ERA-interim reanalysis data showed that enhanced values of OWZ throughout the low- to mid-troposphere provided a robust TC signature. It was found that 95% of TCs in the global IBTrACS TC database could be matched to circulations in the ERA-interim reanalyses containing OWZ values that exceeded 50 and 40 $\times 10^{-6} s^{-1}$ on the 850 and 500 hPa pressure levels respectively at the time of TC declaration, and 90% 24 hours prior to TC declaration. Taking into account imperfect data and non-objective observing practices, these numbers support the hypothesis that enhanced OWZ throughout the low- to mid-troposphere is necessary for TC formation.

| | |
|---|---|
| OWZ (850 hPa) | $60\times10^{-6}s^{-1}$ |
| OWZ (500 hPa) | $50\times10^{-6}s^{-1}$ |
| RH (950 hPa) | 85% |
| RH (700 hPa) | 70% |
| VWS (850—200 hPa) | 12.5 $ms^{-1}$ |
| SH (950 hPa) | 12.3 $gkg^{-1}$ |

**Table 1:** OWZ, relative humidity (RH), vertical wind shear (VWS) and specific humidity (SH) threshold values used in the TC formation predictor.

For use as a TC formation predictor the OWZ thresholds were combined with relative humidity, specific humidity and vertical wind shear thresholds (Table 1), which were tuned in the ERA-interim reanalysis date to best match observed TCs across the global TC basins. A TC was declared if the thresholds were met at non-land locations for three consecutive 24 hour time periods.

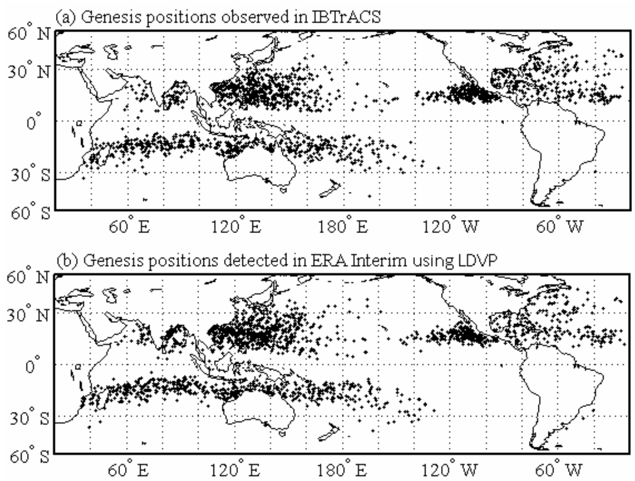


**Figure 2:** Observed (a) and detected (b) TC formation locations, using the OWZ based detector in ERA-interim data from 1989 to 2008.

The 20 year climatology (1989 to 2008), depicted in Fig. 2, shows the OWZ based TC formation predictor (or detector) performs quite well. A closer inspection reveals good representation of interannual variability within TC basins (except the north-Indian), although some biases exist (Fig. 3).

A more rigorous performance assessment tests the ability of the OWZ based predictor to correctly predict each individual storm. Table 2 lists the probability of detection (POD), false alarm rate (FAR), bias and critical success index. POD is the number of correct detections divided by the number of observed storms. FAR is the number of false detections divided by the number of detected storms. BIAS is the number of detected divided by observed storms, and the CSI is the number of correctly detected storms divided by the sum of observed plus false detected storms. There is no reward for correctly detected non-developing systems because there is no non-developing TC database available for verification.

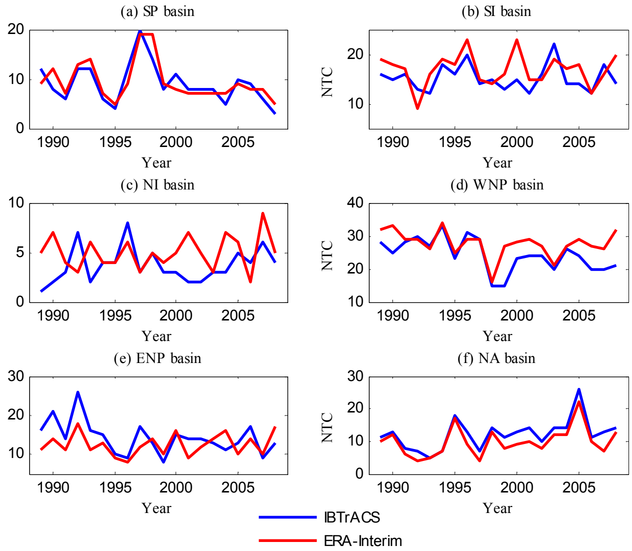


**Figure 3:** Observed (blue) and detected (red) annual TC numbers in (a) South Pacific, (b) South Indian, (c) North Indian, (d) West north Pacific, (e) East north Pacific, and (f) North Atlantic ocean basins.

| Basin | POD | FAR | BIAS | CSI |
|---|---|---|---|---|
| **Global** | 0.78 | 0.25 | 1.04 | 0.62 |
| **SH** | 0.79 | 0.27 | 1.08 | 0.62 |
| **NH** | 0.77 | 0.24 | 1.01 | 0.63 |
| **SP** | 0.74 | 0.29 | 1.04 | 0.57 |
| **SI** | 0.83 | 0.26 | 1.11 | 0.64 |
| **NI** | 0.66 | 0.51 | 1.35 | 0.39 |
| **WNP** | 0.90 | 0.22 | 1.14 | 0.72 |
| **ENP** | 0.70 | 0.20 | 0.88 | 0.59 |
| **NA** | 0.66 | 0.19 | 0.81 | 0.57 |

**Table 2:** Global, hemispheric and basin-wide statistical skill measures, of the OWZ based predictor applied to 20 years of ERA-interim data.

The North Indian Ocean basin performance is poor compared to other basins, with a large over-prediction bias and comparatively low probability of detection and high false alarm rate - a result best summarized in the low CSI. Either there is something unique about TCs in this basin that the detector has not been tuned to recognize, or observation quality or observing practices differ in that basin. The under-prediction in the North Atlantic and East North Pacific may be associated with higher numbers of smaller or shorter lived (border-line) TCs compared with the over-predicted basins of West North Pacific and North Indian Ocean, where formation is often far from land and storms are more likely to be long-lived.

## 4 TC DETECTION IN CLIMATE MODELS

The TC detection algorithm developed and tuned in ERA-interim reanalyses (previous section) was applied to four CMIP3 climate models (CSIRO-Mk 3.5, MPI-Echam5, GFDL 2.0 and GFDL 2.1), without any further tuning or adjustment. The 1970—2000 TC formation climatology is shown in Fig. 4, which shows the models reproduce recent TC climatology reasonably well in most basins with the exception of GFDL 2.0. That model is significantly drier in the lower troposphere than the other models, which means the moisture thresholds are likely to result in the exclusion of many TC-like circulations.

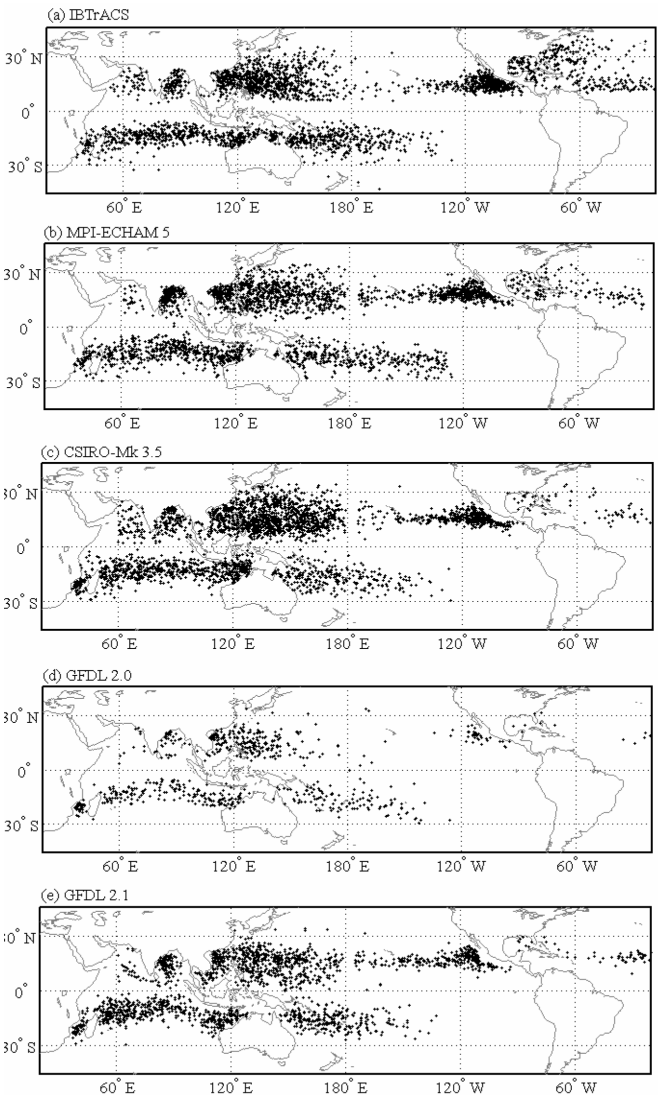


**Figure 4:** 1970—2000 TC formation positions (a) observed, (b) MPI-ECHAM5, (c) CSIRO-Mk3.5, (d) GFDL2.0, and (e) GFDL2.1.

With the OWZ-based detector, all models under-predict TC numbers in the North Atlantic basin, a result consistent with other studies (e.g. Camargo et al. 2005). This issue may be resolution dependent, as some higher resolution models have reported considerable improvement in North Atlantic TC numbers (e.g., Chauvin et al. 2006; Zhao et al. 2009).

## 5 SUMMARY

Simple theoretical arguments are provided that suggest TC formation is most favourable in a vortical environment of zero flow deformation (solid-body rotation), and least favourable in flows with deformation exceeding vorticity. The normalized Okubo-Weiss parameter (Eq. 3) has a value of 1 for solid body rotation and zero when deformation equals vorticity, which makes $OW_{norm}$ an ideal scale parameter for a TC formation index. OWZ is a measure of the absolute vorticity scaled by $OW_{norm}$ (Eq. 7), which is used to identify regions of low-deformation vorticity with the potential to support TC formation. An assessment of TC circulations in 20 years of ERA-interim reanalysis data found that 90% of TCs exhibited elevated OWZ values at both the 850 and 500 hPa pressure levels at least 24 hours prior to TC declaration, a result that supports the hypothesis that enhanced OWZ is necessary for TC formation globally.

An OWZ based TC formation predictor was developed and tuned in ERA-interim reanalysis data that reproduced the observed TC climatology well in all basins except the North Indian Ocean. When applied as a TC detector to a selection of CMIP3 climate models without any further modification, the observed TC climatology was reasonably well reproduced in all but one model.

## ACKNOWLEDGEMENTS

This work was supported by the Pacific Climate Change Science Program.

## REFERENCES

Camargo, S. J., A. G. Barnston, and S. E. Zebiak, 2005: A statistical assessment of tropical cyclone activity in atmospheric general circulation models. *Tellus,* **57A, 589**–604.

Chauvin, F., J. -F. Royer, and M. Déqué, 2006: Response of hurricane-type vortices to global warming as simulated by ARPEGE-Climat at high resolution. *Climate Dyn.,* **27**, 377–399.

Dunkerton, T. J., M. T. Montgomery, and Z. Wang, 2009: Tropical cyclogenesis in a tropical wave critical layer: Easterly waves. *Atmos. Chem. Phys.* 9, 5587—5646.

Holton, J. R., 2004: An introduction to dynamic meteorology. *Elsevier Academic Press*, Burlington, MA., 535 p

Nolan, D. S., 2007: What is the trigger for tropical cyclogenesis? *Aus. Met. Mag.*, **56**, 241-266.

Rozoff, C., W. Schubert, D. Brian, and J. Kossin, 2006: Rapid Filamentation Zones in Intense Tropical Cyclones. *J. Atmos. Sci.*, 63, 325—340.

Shapiro, L. J., and H. Willoughby, 1982: The response of balanced hurricanes to local sources of heat and momentum. *J. Atmos. Sci.,* **39,** 378–394.

Wang, Y., 2008: Rapid Filamentation Zone in a Numerically Simulated Tropical Cyclone. *J. Atmos. Sci.*, 65, 1158—1181.

Zhao, M., M. I. Held, S. -J. Lin, and G. A. Vecchi, 2009: Simulations of Global Hurricane Climatology, Interannual Variability, and Response to Global Warming Using a 50-km Resolution GCM. *J. Climate*, **22**, 6653–6678.